Cell Reports
Article

NPTX1 Regulates Neural Lineage Specification from Human Pluripotent Stem Cells

Nathan C. Boles,[1,4] Sarah E. Hirsch,[1,2,4] Sheila Le,[1] Barbara Corneo,[1,2] Fadi Najm,[3] Andrew P. Minotti,[1] Qingjie Wang,[1] Steven Lotz,[1] Paul J. Tesar,[3] and Christopher A. Fasano[1,2,*]
[1]The Neural Stem Cell Institute, 1 Discovery Drive, Rensselaer, NY 12144, USA
[2]Department of Biomedical Sciences, University at Albany, New York State University of New York, Albany, NY 12201, USA
[3]Department of Genetics, School of Medicine, Case Western Reserve University, Cleveland, OH 44106, USA
[4]These authors contributed equally to this work
*Correspondence: chrisfasano@neuralsci.org
http://dx.doi.org/10.1016/j.celrep.2014.01.026

SUMMARY

Neural induction is the first fundamental step in nervous system formation. During development, a tightly regulated niche modulates transient extracellular signals to influence neural lineage commitment. To date, however, the cascade of molecular events that sustain these signals in humans is not well understood. Here we show that NPTX1, a secreted protein, is rapidly upregulated during neural induction from human pluripotent stem cells (hPSCs). By manipulating its expression, we were able to reduce or initiate neural lineage commitment. A time-course transcriptome analysis and functional assays show that NPTX1 acts in part by binding the Nodal receptor cofactor TDGF1, reducing both Nodal and BMP signaling. Our findings identify one of the earliest genes expressed upon neural induction and provide insight into human neural lineage specification.

INTRODUCTION

During early embryonic development, neural tissue is derived from the ectodermal germ layer. The sequence of events that dictate this process requires a delicate balance and integration of different extracellular signals. The process by which primitive, embryonic ectodermal cells respond to neuralizing signals is known as neural induction and marks the first step in neural lineage commitment. Elegant experiments in lower vertebrates revealed many molecules that are critical for nervous system induction (Weinstein and Hemmati-Brivanlou, 1999), and studies in rodent models have allowed the discovery of additional genes that are crucial for this process (Levine and Brivanlou, 2007). Other investigations have shown that the inhibition of transforming growth factor β (TGF-β) and BMP signaling pathways is the primary mechanism that triggers neural induction in animal models (Hemmati-Brivanlou and Melton, 1994) and human systems (Chambers et al., 2009). Although all of these studies have been invaluable in advancing the field of neural development, the immediate transcriptional events that occur downstream to trigger and sustain neural induction have been less described, particularly in humans. Additionally, a recent study that revealed differences between mice and humans in expression of the neural gene PAX6 in the early developing brain highlighted the need for more comprehensive studies in the human system (Zhang et al., 2010).

Human pluripotent stem cell (hPSC) technology allows us to directly assess the molecular determinants of human nervous system induction and identify critical genetic regulators of this process. Utilizing the knowledge gleaned from lower-animal studies, Chambers et al. (2009) developed a defined dual SMAD inhibition protocol for deriving neural cells from hPSCs. This approach uses a small molecule (SB435412) to inhibit TGF-β signaling and high concentrations of NOGGIN to inhibit BMP signaling. In addition to that study, other groups have also shown that the TGF-β signaling pathway (in particular, Activin/Nodal signaling) is critical for regulating the balance between human embryonic stem cell (hESC) pluripotency and neurectodermal commitment (James et al., 2005; Patani et al., 2009; Smith et al., 2008; Vallier et al., 2004, 2009). The Nodal signaling pathway is regulated at many levels, both extracellularly and intracellularly, and a recent study using hESCs showed that a SMAD-interacting protein can block Nodal signaling and in turn cause neural differentiation (Chng et al., 2010). Extracellularly, Nodal is regulated by a secreted protein, TDGF1 (or CRIPTO), that works as a coreceptor to increase Nodal binding efficiency and overall signal output (Yeo and Whitman, 2001). Blockade of TDGF1 has been shown to induce neurectodermal differentiation in mouse embryos (D'Andrea et al., 2008) as well as mouse embryonic stem cells (mESCs) (Lonardo et al., 2010). Nodal has also been shown to regulate the BMP pathway (Yeo and Whitman, 2001), thus raising the possibility that an extracellular Nodal pathway regulator might also have an effect on the BMP pathway. As extracellular proteins during development play critical roles in initializing and turning down signaling pathways, the identification of extracellular regulators of TGF-β/Nodal signaling will provide critical information about the regulation of hESC pluripotency and neural differentiation.

Using a defined neural induction protocol, we identified NPTX1 as a secreted protein that is transiently released from

differentiating hPSCs and is critical for neural induction. Genetic loss-of-function studies showed that hPSCs exhibit significantly impaired neural cell induction, whereas genetic gain-of-function results in robust, spontaneous neural differentiation. Importantly, the result of robust differentiation could be mimicked by the addition of NPTX1-conditioned media (CM), even in hESCs with genetically low levels of *NPTX1*. Interestingly, molecular analyses revealed that NPTX1 functions, in part, by regulating both Nodal and BMP signaling by binding to TDGF1, a protein that is involved in regulating pluripotency and neural differentiation. Our study identifies and characterizes a molecular mechanism by which hPSCs specify the neural lineage, providing insight into the endogenous regulators of human nervous system lineage commitment.

RESULTS

NPTX1 Reduction Leads to Impaired Neural Induction from hPSCs

To identify novel regulators of the neural induction process, we used a recently developed protocol to derive neural cells from hESCs (Chambers et al., 2009), and inspected the transcriptome throughout the differentiation time course to identify genes that transiently increased in expression during the early stages and were rapidly downregulated before neural characteristics appeared (Fasano et al., 2010). One gene that fits this profile is *NPTX1*, whose expression transiently increased early in neural differentiation from hESCs at mRNA and protein levels (Figures 1A and 1B). This profile was verified in another hESC line, WA-01 (Figure S1A). *NPTX1* is a member of the pentraxin family of proteins, which are secreted, form pentamers and decamers, and can bind to a wide variety of ligands, including bacteria, toxins, carbohydrates, and chromatin (Kirkpatrick et al., 2000). The ability of these proteins to form big protein complexes that can bind chromatin makes them intriguing in the context of early human neural development. *NPTX1* is expressed by adult hippocampal neurons (Cho et al., 2008) with no known function in embryonic development. To assess the functional role of this gene during neural induction, we made three lentiviral small hairpin RNA (shRNA) constructs as previously described (Fasano et al., 2007) and transduced hESCs. Two were successful in reducing *NPTX1* levels by mRNA and protein (Figures S1B–S1D), and lentiviral manipulation did not alter hESC pluripotency markers while they were maintained in conditions favoring pluripotency (Figures S1E and S1F). With the use of these verified constructs, clonal hESC lines were established and differentiated toward the neural lineage. At day 7, the cells were monitored for neural markers PAX6 and SOX1 by quantitative RT-PCR (qRT-PCR) and immunostaining. In addition to these markers, we also looked at the early neuroectodermal markers *GBX2* and *SOX2* by qRT-PCR (Patani et al., 2009). In the *NPTX1* shRNA-treated cells, there was a significant reduction in all neural markers compared with the control (Figures 1C and 1D). Importantly, both the *NPTX1* shRNA that was not effective at reducing *NPTX1* levels and a scrambled control did not alter neural induction as indicated by *PAX6* expression (Figures S1B and S1G). To verify *NPTX1*'s role in other pluripotent lines, we differentiated bona fide induced PSCs (iPSCs) generated in the lab (Figures S2A and S2B) toward the neural lineage and assessed *NPTX1* expression. Similar to our findings in hESCs, we observed a transient increase in *NPTX1* preceding the increase of the neural marker PAX6 (Figure S2C). Using shRNA, we reduced the levels of *NPTX1* in the iPSCs and differentiated them toward the neural lineage. We found reduced levels of *PAX6* mRNA after 7 days, consistent with hESC results (Figure S2D).

In addition to the marker analysis, we picked hESC-derived neural cells from each condition at day 9 and placed them in neurosphere (NS)-forming conditions to identify neural progenitor cells (NPCs) (Reynolds and Weiss, 1992). As expected, robust NS generation was identified in the control group, but the shRNA condition had significantly less NS generation, supporting the idea that *NPTX1* is important for neural induction (Figure 1E). It was possible that *NPTX1* regulated the proliferation of already established precursors, and the reduction of NSs was the result of reduced NPC proliferative capacity. To determine whether *NPTX1* knockdown was decreasing the proliferation of already specified precursors, NSs were grown for 1 week, passaged, and then transduced with a control or *NPTX1* shRNA lentivirus. After 7 days of culture, there was no difference in the number of NSs compared with the control, suggesting that *NPTX1* is important for neural induction, but not for neural precursor proliferation (Figure 1F). In addition to NS number, we also looked at NS size, as smaller spheres might indicate a proliferation defect. In the *NPTX1* shRNA cells, there was no significant difference in NS size compared with the control (Figure 1F). Finally, both control and shRNA hESCs were differentiated toward the neural lineage, and at day 9 a cell-cycle analysis was performed to rule out a proliferative defect. No significant difference was identified (Figure 1F).

It was also possible that *NPTX1* regulated the general differentiation potential of hPSCs, and knocking it down would inhibit its ability to differentiate into any lineage—not just neural. To test this, we differentiated hESCS treated with *NPTX1* shRNA toward endodermal and mesodermal fates as previously described (Kennedy et al., 2007; Nostro et al., 2011). For the mesoderm, we found that *NPTX1* shRNA cells were able to give rise to *Brachyury*-expressing cells (as determined by qRT-PCR) as well as KDR+ cells (as determined by flow analysis), indicating a mesodermal fate (Figure 1G). Interestingly, the *NPTX1* shRNA cells had higher percentages of the mesodermal populations compared with the control. Upon endoderm differentiation, NPTX1 shRNA cells expressed the endodermal marker *SOX17* (by qRT-PCR) as well as CXCR4+ cKit+ cells (by flow cytometry), indicating that both the *NPTX1* shRNA and control cells gave rise to endoderm (Figure 1H). At no time point measured for either mesodermal or endodermal differentiation did we find expression of *PAX6*, indicating that neural differentiation had not occurred. These data suggest that *NPTX1* is upregulated prior to neural differentiation, and its reduction leads to a deficit in neural induction from hPSCs.

To test whether *Nptx1* regulates mouse neural induction, we differentiated pluripotent mouse epiblast stem cells (mEpiSC) (Tesar et al., 2007) to the neural lineage and looked at *Nptx1* expression over the time course. Neural differentiation occurs much faster in mice, with neural characteristics appearing between days 3 and 5 (Najm et al., 2011). To ensure that we could identify a similar transcriptional event in mice, we looked as early as 24 hr after differentiation for expression of *Nptx1*. In contrast

Cell PRESS
Open ACCESS

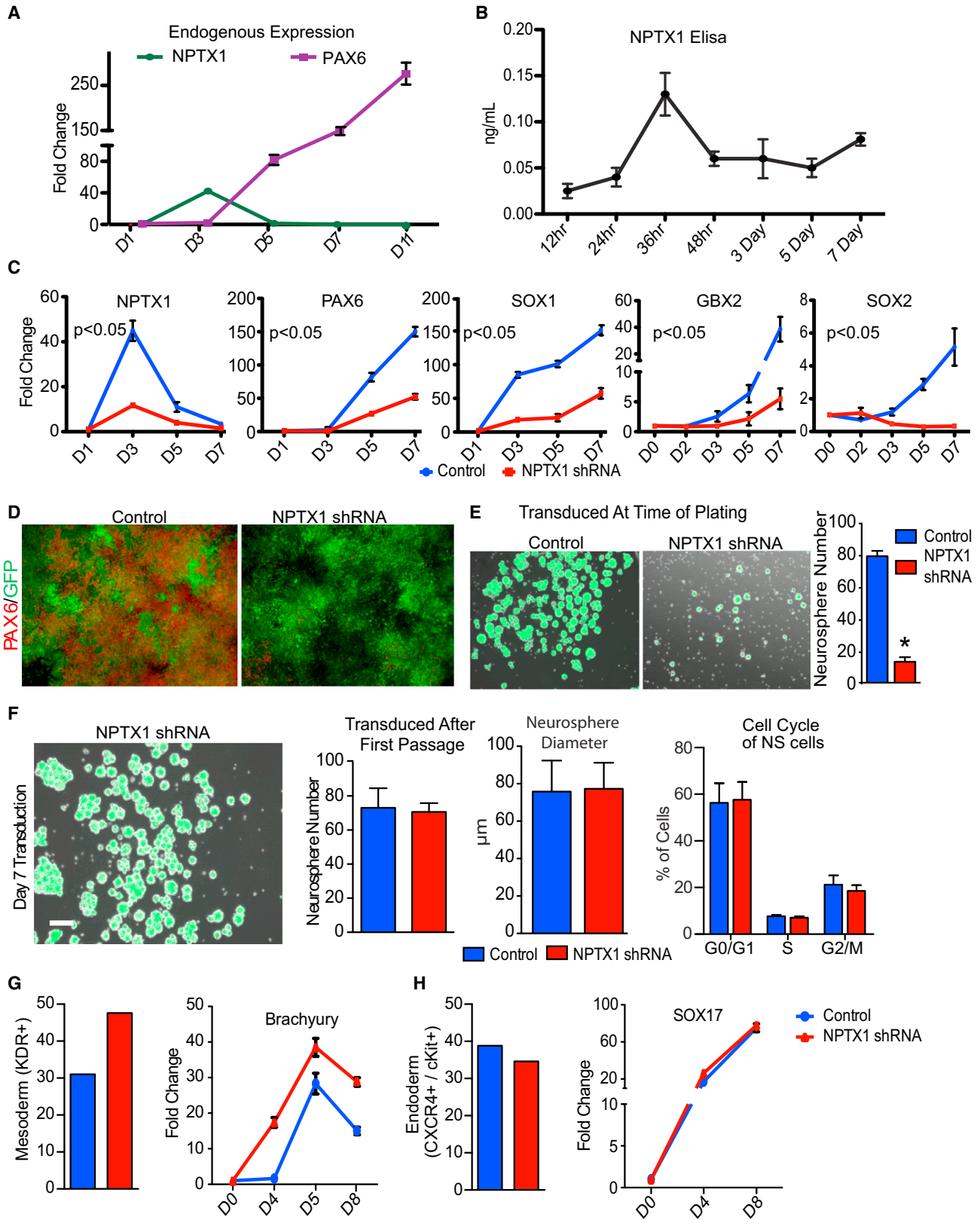

(legend on next page)

to what was observed in the human system, *Nptx1* did not significantly increase until the neural lineage was already established (day 4), suggesting that in mice it may not serve as an inducer of neural fate (Figure S3A). To test NPTX1 functionally in this context, we transduced mEpiSC with *NPTX1* shRNA and differentiated them to the neural lineage. Although a significant reduction in *NPTX1* was observed, the ability to make neural cells was not altered, as indicated by expression of the mouse neural markers *Sox2* and Nestin (Figure S3B). Therefore, these examples show that *NPTX1* gene expression does not precede that of neural identity in the mouse, and suggest a possible difference between the mouse and human systems.

NPTX1 Expression Enhances Neural Induction from hPSCs

To test whether NPTX1 would enhance neural induction, we used a lentiviral vector to force expression in hESCs. We differentiated these cells, along with a control-transduced line, to the neural lineage and analyzed them at four time points. As seen in the control, *NPTX1* expression peaked early, about the time the pluripotency gene *NANOG* began to drop, and then rapidly decreased before the neural markers PAX6 and SOX1 turned on (Figure 2A). In the *NPTX1* overexpression condition, *NPTX1* levels were elevated from day 1, *NANOG* expression decreased more rapidly, and *PAX6* and *SOX1* levels were increased earlier and to a higher extent, as shown by qRT-PCR (Figure 2A). This effect was confirmed by immunostaining that showed 57.2% PAX6+ cells at day 5, compared with 24.6% in the control (Figure 2B). Additionally, a dramatic reduction of NANOG was seen by day 5 compared with the control, which still exhibited robust staining (Figure 2B). These data show that *NPTX1* accelerates pluripotency exit and neural differentiation from hESCs under directed differentiation conditions.

We then examined whether *NPTX1* alone would be able to drive neural differentiation. *NPTX1*-transduced hESCs were allowed to spontaneously differentiate in a base cell culture medium without added growth factors. The sustained levels of *NPTX1* led to a more robust differentiation to PAX6+ cells compared with the control and shRNA-treated cells (Figure 2C). Additionally, *Brachury* and *SOX17* levels were lower in the *NPTX1*-overexpression condition compared with the control, suggesting a preferential differentiation to the neural lineage (Figure 2C). The neural cells generated via *NPTX1* overexpression also expressed the neural markers *SOX2* and *Nestin* (Figure 2D).

NPTX1 is a secreted protein, and to determine whether it is capable of autocrine or paracrine neural induction, we transduced 293 kidney cells with *NPTX1* overexpression or control vector and harvested the CM from each. To verify protein expression, we added the CM to hESCs for 24 hr and fixed them for protein analyses. Using an NPTX1 antibody, we observed few NPTX1-positive cells in control CM-treated hESCs, whereas the NPTX1-CM treated cells were now 59% positive for NPTX1. To test the effects of secreted NPTX1, hESCs were placed in both types of CM and left to differentiate spontaneously for 7 days. Cells that were treated with the control CM differentiated into few neural cells, whereas those that received NPTX1 CM exhibited a neuroepithelial morphology (Figure 2E), robustly generated PAX6+ neural cells (Figure 2F), and had lower levels of NANOG (Figure 2G). This result was dose dependent, as dilutions of NPTX1 CM resulted in decreasing amounts of neural induction indicated by PAX6 expression. Interestingly, anything less than a 25% dilution did not induce the neural lineage (Figure 2H). To confirm that this effect was specific to *NPTX1*, we differentiated hESCs with NPTX1 CM in the presence of an NPTX1 blocking peptide. In this context, neural induction was severely inhibited (Figure 2H). In addition, we added NPTX1 CM to *NPTX1* shRNA differentiating hESCs and were able to rescue the loss of neural cells (Figure 2I). These data suggest that *NPTX1* alone can drive neural differentiation robustly in hESCs without the addition of other exogenous factors.

To test the strength of *NPTX1* for driving differentiation toward neural lineages, we attempted to derive both endoderm and mesoderm in the *NPTX1*-overexpressing cells. Using flow cytometry and qRT-PCR, we found that *NPTX1*-overexpressing cells were able to differentiate into both mesoderm and endoderm (Figures 3A and 3B). However, in both differentiation protocols, the *NPTX1*-overexpressing cells also gave rise to neural cells, as measured by PAX6 expression. This result shows that even when *NPTX1*-overexpressing cells are driven to produce mesoderm and endoderm, they still produce a considerable number of neural cells, indicating that NPTX1 exposure strongly drives neural induction in hPSCs.

Loss of *NPTX1* Maintains the Pluripotency Program during Directed Neural Differentiation

To understand the mechanism of *NPTX1*-mediated neural differentiation, we obtained high-resolution temporal gene-expression profiles at five time points during the neural induction protocol (Figure 4A). Global gene-expression studies were

Figure 1. NPTX1 Is Critical for Human Neural Induction

(A) Time course of *NPTX1* expression during neural differentiation. qPCR showed a transient increase in *NPTX1* expression preceding that of the neural marker PAX6.

(B) Transient NPTX1 expression was confirmed at the protein level by ELISA.

(C) Time course of neural differentiation, showing a decrease in the expression of the key neural genes *PAX6*, *GBX2*, *SOX2*, and *SOX1* by qRT-PCR in *NPTX1* shRNA-expressing cells.

(D) *NPTX1* shRNA was shown to inhibit neural cell differentiation by immunostaining for PAX6 (red) and GFP (green).

(E) Cells isolated at day 9 of neural differentiation from *NPTX1* shRNA hESCs give rise to fewer NSs (quantified on the right). Scale bar, 100 μm; *$p < 0.05$; $n = 3$.

(F) hESCs were differentiated to neural cells, and at day 9 cells were picked and transduced with control or *NPTX1* shRNA lentivirus. After 7 days there was no difference in NS formation, NS size, or cell cycle (quantified on the right). Scale bar, 100 μm; *$p < 0.05$, **$p < 0.001$; $n = 3$.

(G and H) *NPTX1* shRNA hESCs were differentiated toward mesoderm or endoderm. Flow cytometry examining differentiating cells for KDR expression showed an increase in mesoderm lineage cells in the *NPTX1* shRNA-treated cells versus control cells. qRT-PCR for mesoderm showed increased expression of Brachyury, whereas the endodermal marker Sox17 exhibited levels similar to the control. In addition, flow analysis for endoderm induction shows similar expression of cKit and CXCR4 in control and *NPTX1* shRNA-treated cells.

All error bars are SEM. See also Figures S1–S3.

Cell PRESS
Open ACCESS

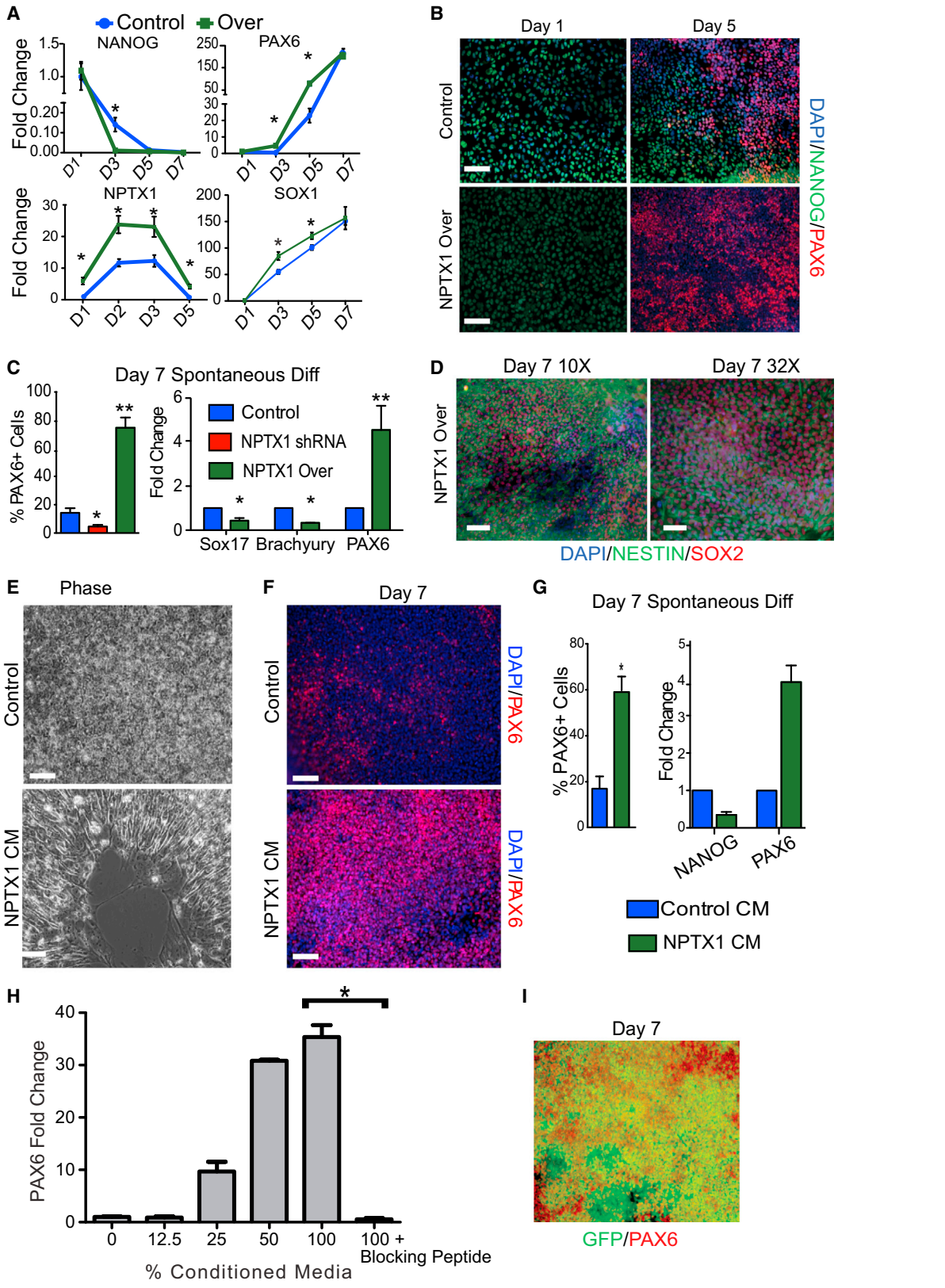

(legend on next page)

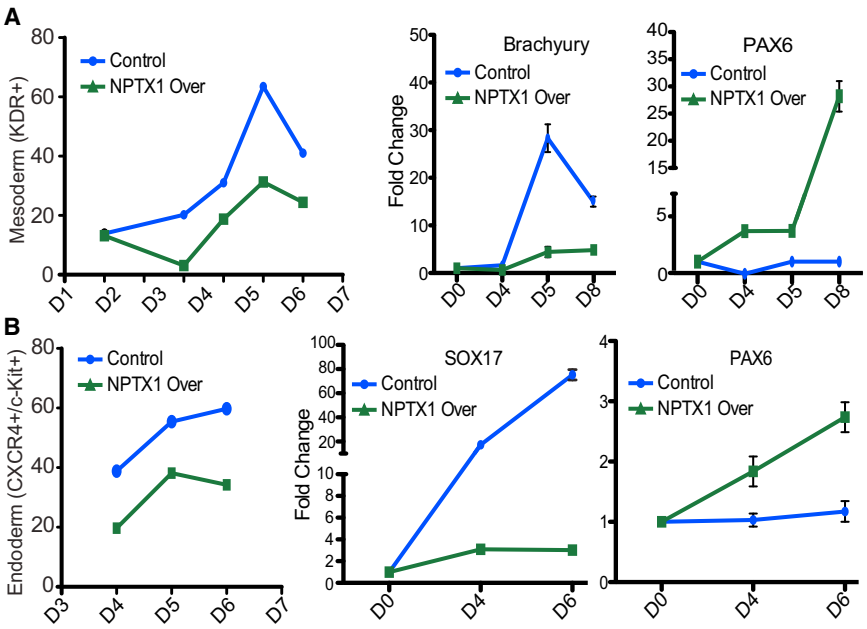

Figure 3. *NPTX1*-Overexpressing Cells Give Rise to Neural Cells when Differentiated to Other Lineages

NPTX1-overexpressing (*NPTX1* Over) cells were differentiated toward mesodermal or endodermal lineages using established protocols.

(A) *NPTX1* Over cells differentiated into mesoderm lineage cells at a lower rate than control cells. In addition, qRT-PCR showed lower levels of *Brachyury* (mesoderm) and high levels of *PAX6* (neural lineages), indicating that the *NPTX1* Over cells were still deriving a hefty population of neural cells as well.

(B) *NPTX1* Over cells differentiated to endodermal cells, albeit at a lower rate compared with control cells, as measured by CXCR4 and cKit positivity using flow cytometry, and by *SOX17* expression measured by qRT-PCR. Once again, higher expression of *PAX6* was observed.

All error bars are SEM. See also Figure S1.

carried out in three independent samples for each time point and culture condition. We analyzed the data for genes with significant changes in their expression profiles by regressing the normalized expression values using polynomial least-squares regression, and performing an ANOVA on the coefficients of regression to identify genes with significant changes and at least a 2-fold difference between their high and low expression over the time course for each group. Genes with significant changes were then divided into three groups: genes that changed in the control and *NPTX1* shRNA cells (Table S1), genes that were unique to the control cells (Table S2), and genes that were unique to the *NPTX1* shRNA cells (Table S3). Approximately 2,100 genes changed in the control cells during this time course; however, only 955 genes changed expression in the *NPTX1* shRNA condition, and roughly 701 of those genes also changed in the control condition (Figure 4B). For a global view of the changes specific to each condition, we undertook an enrichment analysis to find gene categories in which the genes that were unique to either the control or *NPTX1* shRNA cells were enriched. Notably, Gene Ontology (GO) categories dealing with development of various tissues and cell differentiation, including neural and brain development, were greatly enriched in the control cells, whereas in the *NPTX1* shRNA cells, these categories were either not enriched or were depleted (Figure 4C; Tables S4 and S5). Furthermore, the *NPTX1* shRNA expression profile showed enrichment for genes involved in pluripotency (Table S6) when compared with the control expression profile. In particular, genes such as OCT-4 and E-Cadherin failed to reduce over time as they do in control hESCs during neural differentiation. This was confirmed by qRT-PCR (Figure 4D). Among the transcripts that were decreased in *NPTX1* shRNA-treated versus control cultures at day 7 of differentiation, we found genes associated with neural development (e.g., *PAX6* and *EMX2*; Table S2), as confirmed by qRT-PCR (Figure 4E). Together, these data confirm our previous experiments showing that *NPTX1* shRNA reduces neural lineage commitment from hESCs, and suggest that *NPTX1* is a critical regulator of pluripotency versus neural commitment.

Figure 2. *NPTX1* Is Adequate for Human Neural Induction

(A and B) hESCs overexpressing *NPTX1* were differentiated toward the neural lineage, resulting in accelerated pluripotency exit (NANOG) and neural commitment (*PAX6* and *SOX1*), as shown by (A) qRT-PCR (*$p < 0.05$, n = 3) and (B) immunocytochemistry. Scale bar, 100 μm.

(C) hESCs transduced with control, *NPTX1* shRNA, or *NPTX1*-overexpression viruses were spontaneously differentiated in a KSR base medium. Few PAX6+ cells were seen in the control and significantly fewer were seen in the shRNA condition, whereas *NPTX1*-overexpressing cells robustly generated PAX6+ cells. The left graph shows the percentage of PAX6+ cells in each condition. The right graph shows the mRNA levels of genes associated with all three germ layers (*SOX17*, endoderm; *Brachyury*, mesoderm; and *PAX6*, neural ectoderm). *$p < 0.05$, **$p < 0.001$, n = 3.

(D) The resulting neural cells also express SOX2 and NESTIN. Scale bars, 100 μm and 50 μm.

(E–G) NPTX1 CM from transduced fibroblasts can induce neural cells from hESCs.

(E) At 5 days after NPTX1 CM addition, neuroepithelial-like cells were observed along with emerging PAX6+ cells.

(F) By day 7, a significant number of the cells present are PAX6+. Scale bar, 200 μm.

(G) Quantification of PAX6+ cells and mRNA levels of *NANOG* and *PAX6* in the CM experiment. *$p < 0.05$, n = 3.

(H) Quantification of the CM experiment showing that increasing levels of CM result in increased PAX6 levels, and the rescue using the blocking peptide (*$p < 0.05$).

(I) The NPTX1 CM was added to *NPTX1* shRNA hESCs and was able to rescue the neural induction deficit when these cells were differentiated. GFP is a marker of shRNA cells, PAX6 marks neural cells. Scale bar, 200 μm.

All error bars are SEM. See also Figures S1 and S6.

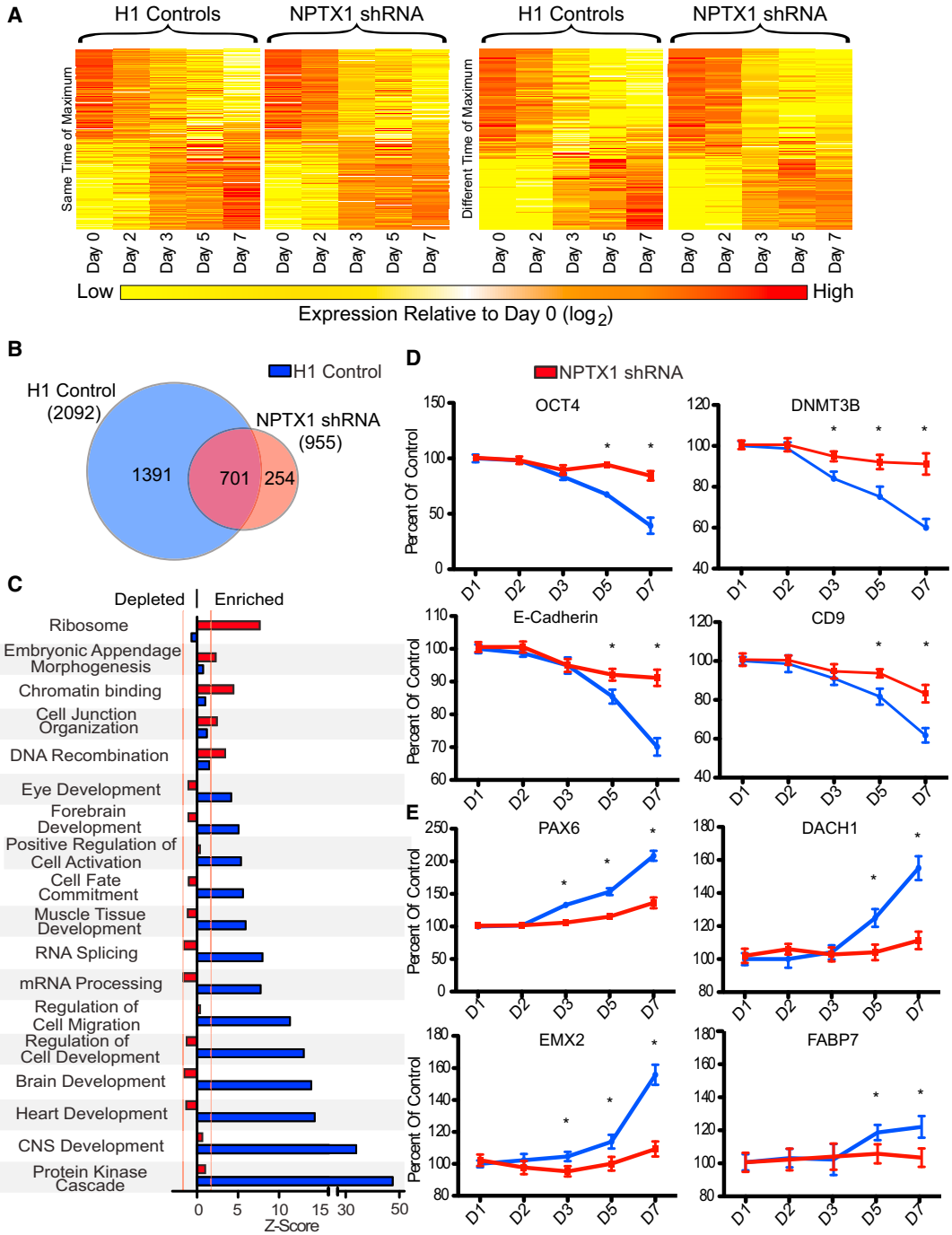

Figure 4. Expression Profiling Reveals that *NPTX1* shRNA Cells Are Delayed in Pluripotency Exit

(A) Heatmaps showing the expression-level fluctuations of significantly changing genes in both control and *NPTX1* shRNA cells over the time course. The heatmaps on the left show genes with the same time of maximum (TOM) between the control and *NPTX1* shRNA cells, and the heatmaps on the right show genes with different TOMs.

(B) Venn diagram describing the number of genes that changed in each condition and their relation to each other.

(C) GO enrichment analysis of genes that changed significantly over the time course and were unique to either control or *NPTX1* shRNA cells reveals a pattern of enrichment for development categories in control cells and a lack of enrichment of those categories in the *NPTX1* shRNA cells. Significant changes cross the orange thresholds.

(D and E) Real-time PCR of a select set of hESC maintenance genes (D) and genes involved in neural differentiation (E) shows a clear difference between control cells and the *NPTX1* shRNA cells. *$p < 0.05$, $n = 3$.

All error bars are SEM. See also Tables S1, S2, S3, S4, S5, and S6.

NPTX1 Binds TDGF1 and Negatively Regulates Nodal Signaling

To investigate *NPTX1*'s role in pluripotency, we looked for pluripotency genes that uniquely changed in the control cells, and identified *TDGF1*, an essential positive regulator of Nodal signaling, which decreased in expression during the time course (Figure 5A). Nodal-TDGF1 signaling activates SMAD2/3 and in turn NANOG expression, maintaining hESC pluripotency (James et al., 2005; Vallier et al., 2009), and loss of Nodal signaling has been shown to be an essential signal for neural induction (Patani et al., 2009; Smith et al., 2008). *TDGF1* has been identified both in the extracellular space, as a secreted protein, and in glycosylphosphatidylinositol linked to the membrane, where it interacts with the Nodal receptor. TDGF1 interacts with ALK4, the Nodal receptor, to permit Nodal to bind to the receptor complex, leading to SMAD2 phosphorylation (Yeo and Whitman, 2001).

To understand how TDGF1 was affected by NPTX1 manipulation, we first used qRT-PCR to look at *TDGF1* expression along the neural differentiation time course. We found that, compared with the control, *TDGF1* expression was significantly higher 7 days after differentiation in the *NPTX1* shRNA-treated cells (Figure 5A). This was also true for *SMAD2/3* and *NANOG*, suggesting that NPTX1 may be regulating the Nodal pathway via TDGF1 (Figure S4A). To confirm this, we looked next at the NPTX1 amino acid sequence and compared it with key regulators of the Nodal pathway. Interestingly, NPTX1 shares a striking homology to LEFTY, a secreted antagonist of the Nodal pathway. Lefty has been shown to modulate Nodal signaling by binding to TDGF1, rendering Nodal signaling inactive (Chen and Shen, 2004). To investigate whether NPTX1 works in a fashion similar to that observed for LEFTY, we performed coimmunoprecipitation (coIP) for TDGF1 and NPTX1 using the culture media from differentiating hESCs. Indeed, NPTX1 could be pulled down along with TDGF1, suggesting that NPTX1 binds TDGF1 extracellularly, inhibiting its ability to bind to the Nodal receptor (Figure 5B). We next asked whether high levels of NPTX1 in the extracellular space would reduce the amount of TDGF1 present at the cell surface. CM from NPTX1-expressing cells was harvested along with control media and added to hESCs 1 hr before fixation. Looking only at the cell surface, in the control condition there were high levels of TDGF1 and low levels of NPTX1 staining—a condition favorable to pluripotency. In the conditions with NPTX1 CM, a much-reduced TDGF1 expression was observed at the cell surface along with higher NPTX1 (Figure 5C). Finally, we made an NPTX1-His-tagged vector and used it to make a CM containing NPTX1-His. We applied this medium to hESCs for 1 hr and performed a coIP on the membrane fraction of the lysed cells, and were able to pull down TDGF1 with the NPTX1-His protein (Figure 5B). Together, these data suggest that NPTX1 binds TDGF1 on the cell surface, as well as in the extracellular space, providing a mechanism for how NPTX1 could modulate Nodal signaling.

To investigate this functionally, we looked at the nuclear expression of SMAD2/3 in control and NPTX1-expressing hESCs as a readout of active Nodal signaling. Undifferentiated hESCs showed a high level of nuclear SMAD2/3 expression, and during spontaneous differentiation, there were similar levels of nuclear SMAD2/3 after 3 days. However, in the spontaneously differentiating *NPTX1*-expressing hESCs, there was a dramatic decrease in nuclear SMAD2/3 expression after 3 days (Figure 5D). The same was observed for NANOG expression (Figure S4B). These data suggest that *NPTX1* modulates the Nodal pathway and the downstream pluripotency program. To further verify whether TDGF1 is involved in NPTX1-mediated neural induction, we added a TDGF1 blocking antibody into the *NPTX1* shRNA condition. When TDGF1 was blocked, neural induction could proceed normally in the *NPTX1* shRNA cells, suggesting that NPTX1 increases neural induction in part by binding TDGF1 and reducing Nodal signaling (Figure 5E).

NPTX1 Expression Reduces BMP signaling

Secreted proteins expressed during development have been shown to inhibit multiple signaling pathways. Cerberus is a secreted protein that has been shown to inhibit both the Nodal and BMP pathways (Piccolo et al., 1999). The directed neural differentiation paradigm used in this study employs both TGF-β and Noggin blockers, because it was originally shown that blocking only TGF-β was not sufficient to drive neural commitment (Chambers et al., 2009). Although TDGF1 works to enhance Nodal signaling, it has been shown that Nodal itself can bind up BMPs and thus lower BMP signaling (Yeo and Whitman, 2001). Because NPTX1 depletes available TDGF1 in the extracellular space and cell surface, it seemed plausible that the excess Nodal could now dampen BMP signaling. To test whether *NPTX1* expression can reduce BMP signaling, we employed the dual SMAD protocol to generate neural cells. In one condition, we substituted *NOGGIN* for a TDGF1 blocking antibody to see whether TDGF1 loss could result in robust neural differentiation. As a positive control for BMP signaling, one group was treated with high levels of BMP7. After 7 days of differentiation, we looked at neural marker expression and SMAD1 levels (Figures 6A and 6B). As expected, the dual SMAD inhibition led to robust PAX6 expression and negligible levels of pSMAD1. hESCs treated with BMP7 or SB431542 (TGF-β antagonist) alone gave rise to few PAX6 cells and exhibited high pSMAD1 levels. When SB431542 was combined with the TDGF1 blocking antibody, robust PAX6 expression was observed along with low levels of SMAD1. Finally, the TDGF1 blocking antibody alone gave high PAX6 expression and lowered SMAD1 levels similar to those observed with dual SMAD inhibition and NPTX1 overexpression. Together, these data indicate that NPTX1 increases neural induction in part by reducing BMP signaling via TDGF1 regulation.

DISCUSSION

Our study implicates a role for the pentraxin family of proteins in regulating human nervous system development. Although functional studies of *NPTX1* in the adult mouse brain have linked it to regulating synaptic transmission, no evidence for it regulating neural development has been shown. Interestingly, an *Nptx1* null mouse was made in a previous study and no neural induction deficits were identified (Bjartmar et al., 2006). Our data show that as mouse PSCs differentiate,

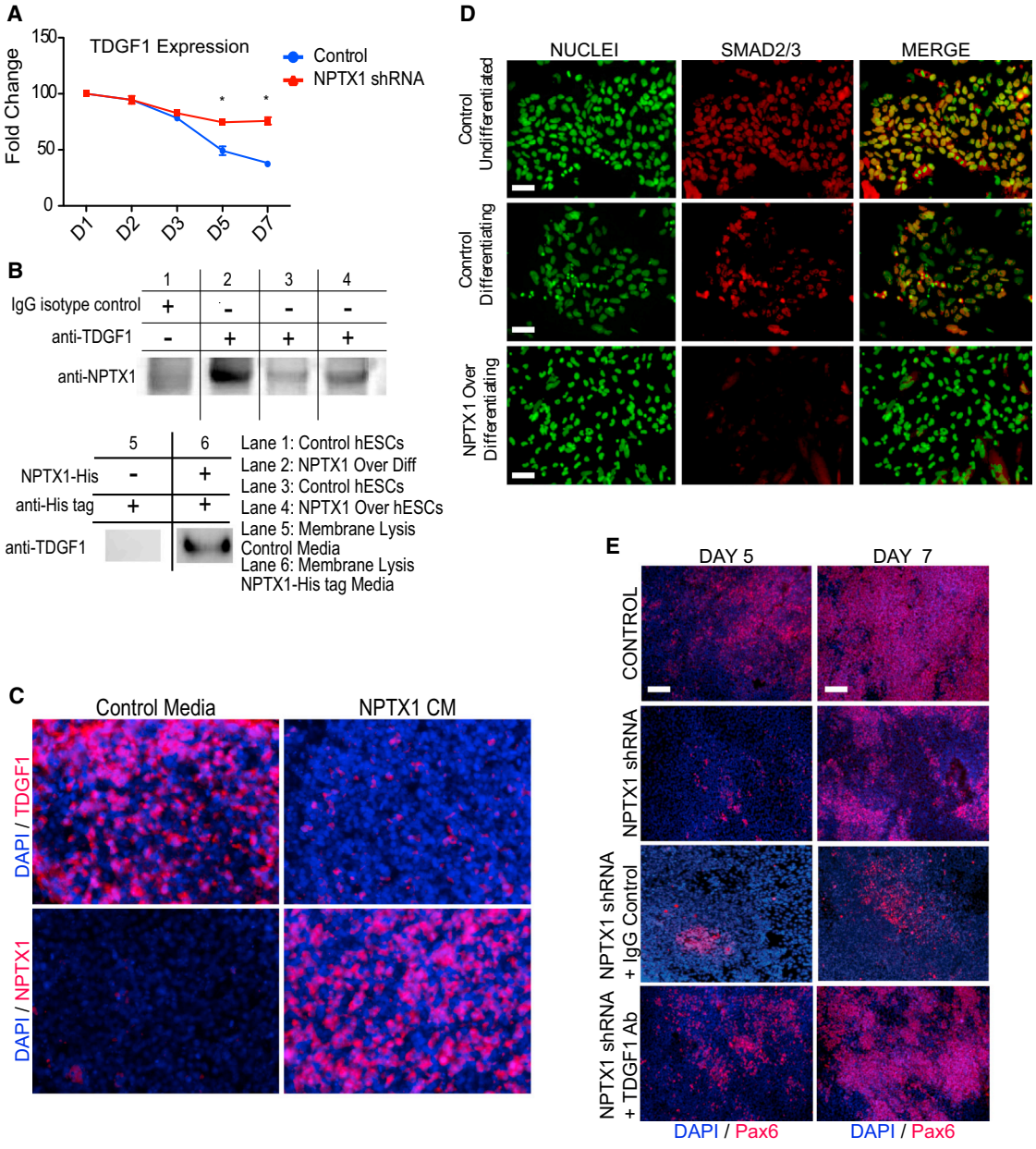

Figure 5. NPTX1 Binds TDGF1, Blocking Nodal Signaling to Induce Neurectoderm

(A) Upon neural differentiation, *TDGF1* expression is rapidly downregulated, but this is abolished in the *NPTX1* shRNA condition. *$p < 0.05$, $n = 3$.

(B) Using coIP, we were able to show that in spontaneously differentiating hESCs, NPTX1 can bind TDGF1 in the extracellular space. Using His-tagged NPTX1 media, we were also able to demonstrate that NPTX1 binds membrane-bound TDGF1 by coIP as well.

(C) Cells were treated with either control media or NPTX1 CM for 1 hr and stained for TDGF1 or NPTX1.

(D) Overexpression of *NPTX1* leads to a rapid loss of nuclear SMAD2/3 upon differentiation. Scale bar, 50 μm.

(E) The addition of TDGF1 binding antibody rescues the neural differentiation deficit seen in the *NPTX1* shRNA condition. Scale bar, 200 μm.

All error bars are SEM. See also Figures S4 and S5.

NPTX1 is not expressed until neural markers appear, whereas in humans, *NPTX1* expression precedes the expression of neural markers. Additionally, knockdown of *NPTX1* in mEpiSCs did not affect their ability to induce neural cells. The discrepancy between the mouse and our human data could be due to many factors. First, *NPTX1* could have different functions in mice and humans. Recently, a study revealed that the first marker to be expressed in the human neural plate is *PAX6*, not *SOX1*, whereas the opposite is true in mice, with *Sox1* preceding the expression of *Pax6* (Zhang et al., 2010). This finding suggests that the beginning of neural commitment is different in mice compared with humans, raising the possibility that

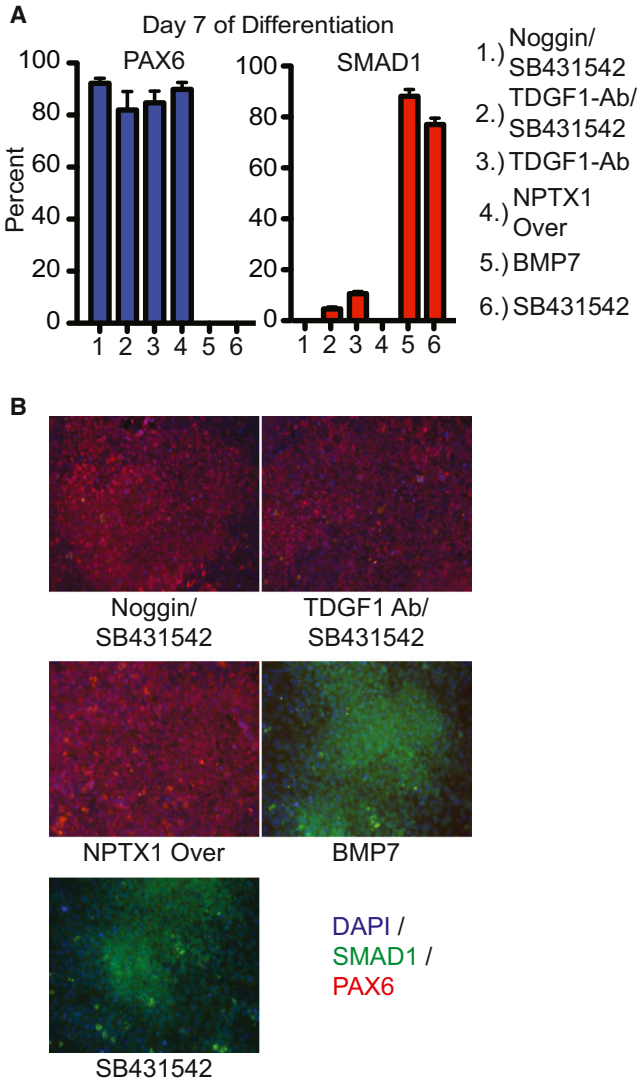

Figure 6. *NPTX1* Indirectly Dampens BMP Signaling

(A) hESCs were driven to differentiate by (1) the Chambers et al. (2009) protocol, (2) TDGF1 blocking antibody (TDGF1-Ab) + SB431542, (3) TDGF1-Ab, (4) NPTX1 overexpression, (5) BMP7 (control), and (6) SB431542. Cells were then examined for PAX6 and SMAD1 expression by immunofluorescence. TDGF1-Ab demonstrated results similar to those obtained by NPTX1 overexpression and the Chambers et al. neural differentiation protocol. In addition, TDGF1 blocking antibody is a reasonable substitute for Noggin to inhibit BMP signaling, as measured by SMAD1 in the Chambers et al. protocol. SB431542-alone-treated cells and BMP7-treated cells showed no PAX6+ cells.

(B) Cells from each condition stained for PAX6 and SMAD1.

All error bars are SEM.

NPTX1's role in neural development might be confined to the human system. Another possible explanation for the differences revealed by *NPTX1* shRNA knockdown compared with the *Nptx1* knockout is that the knockout mouse has developed compensatory mechanisms that enable neural development to proceed normally. The shRNA studies reveal the effects of acute gene loss, which do not allow a substantial amount of time for a compensatory mechanism to develop. Previous studies have shown differences in the role of proteins using knockout versus shRNA (Blagosklonny, 2004; Fasano et al., 2007). More studies comparing *NPTX1*'s role in mouse versus human neural induction need to be carried out before concrete conclusions can be made.

An important finding in our study is *NPTX1*'s dual mechanism of action. Classically, it was shown that blockade of both Activin/Nodal and BMP signals was necessary for neural induction (Casellas and Brivanlou, 1998). This was mimicked in a later study with hESCs using dual SMAD inhibition (Chambers et al., 2009). In this study, when the BMP antagonist *NOGGIN* was omitted, trophectoderm (a BMP-dependent lineage) was generated as opposed to neural cells. However, some reports in the literature suggest that blockade of only the Activin/Nodal component is enough to enhance neural differentiation from hESCS (Patani et al., 2009). The inconsistency in these results might lie in the culture medium used in the two studies. The former study used a medium containing the supplement knockout serum replacement (KSR), whereas the latter used a very defined medium with no KSR. There have been studies looking specifically at the cell-signaling effects of media containing KSR, and it was found to have a strong BMP component (Xu et al., 2005). When hESCs are differentiated in an environment where basal BMP signaling is higher, blockade of this signal might be required for neural commitment to proceed. In the dual SMAD protocol, the Nodal signal is blocked by the drug SB43152, which prevents ALK4 phosphorylation and thus signal transduction. However, this drug does not prevent the Nodal ligand from binding its receptor. Our data show that NPTX1 reduces Nodal signaling by binding to a coreceptor, TDGF1. Therefore, NPTX1 does not employ the same method as SB431542 to block signaling. TDGF1 and Nodal bind in the extracellular space and then move to the membrane or bind at the cell surface for signal transduction. If less TDGF1 is present, less Nodal will be at the receptor and it will be free to perform other functions, such as binding to BMPs and preventing receptor activation (Yeo and Whitman, 2001).

Interestingly, when the *NPTX1* shRNA hESCs were differentiated into the mesoderm lineage, a significant increase of mesodermal cells was identified. Mesoderm is a BMP-dependent lineage, and this finding fits with the idea that NPTX1 expression will decrease BMP signaling due to a loss of TDGF1. When NPTX1 levels are reduced, the Nodal-TDGF1 signaling cascade is enhanced, allowing for less available Nodal to bind to BMPs. Along the same lines, it has been shown that dual SMAD blockade leads to commitment of neural cells with an anterior identity (Chambers et al., 2009), whereas blocking only the Activin/Nodal component converts neural cells to a posterior identity (Patani et al., 2009). When neural cells are generated by *NPTX1* expression, they express markers such as *OTX2* and *FOXG1* (Figure S5) just like cells derived by dual SMAD inhibition, thus confirming the idea that NPTX1 blocks both Nodal and BMP signals via TDGF1 inhibition.

Anterior neural cells are generated first in vivo and in vitro, and we wondered whether this could somehow be encoded by

NPTX1. To test this, we used a modified dual SMAD inhibition protocol to generate a posterior neurectoderm and looked at *NPTX1* in this process. Just as in the anterior protocol, *NPTX1* was expressed at the same time during the posterior differentiation protocol (data not shown). This finding suggests that *NPTX1* expression is specific to neural induction and does not confer anterior identity to the neural cells. It will be interesting to investigate the key transcriptional events responsible for anterior versus posterior patterning.

Regulation of the choice between pluripotency and differentiation requires a delicate balance of signals that must be tightly regulated. A recent study highlighted this point by looking at how Activin/Nodal signaling can regulate both pluripotency and endodermal differentiation (Brown et al., 2011). Data from our study indicate that NPTX1 reduces Nodal signaling and in turn pluripotency genes such as *NANOG*. It is worth noting that we identified *NPTX1* by using dual SMAD inhibition for 3 days, and therefore *NPTX1* expression may be secondary to pluripotency exit and work by enhancing an already present *Nodal* blockade while dampening BMP signaling. Because signals in development are transient, *NPTX1* may be one of the first downstream effectors of neural induction ultimately leading to neural lineage commitment. Interestingly, when hESCs are left to spontaneously differentiate by fibroblast growth factor 2 (FGF-2) withdrawal, neural cells are generated at a low frequency. In this paradigm, *NPTX1* expression still turns on, albeit at a much a lower level than when directed to the neural lineage (data not shown). Also, in the hESC control cell line, exogenous dual SMAD inhibition after day 3 does not result in increased *PAX6*, whereas in the *NPTX1* knockdown line, the trend is an increase in *PAX6* when dual SMAD is added for longer than 3 days. This difference could be attributed to the lack of endogenous regulation in the *NPTX1* knockdown line. Neural conversion is completely dependent upon the exogenous dual SMAD block; thus, the more the signal is present, the more neural induction is achieved, albeit always at lower levels compared with the control (Figure S6). These data suggest that a critical level of *NPTX1* expression might be needed to drive a complete neural conversion from hPSCs. This is also echoed in our dose-response CM experiment showing that after 3-fold dilution, neural induction is no longer achieved.

In conclusion, we have identified a member of the pentraxin protein family, *NPTX1*, as a critical regulator of neural lineage commitment from hPSCs. We propose a model in which pluripotency exit leads to the expression and secretion of NPTX1, which then binds and inhibits TDGF1 in the local environment. The result of this action maintains a loss of Nodal and BMP signaling, leading to neural differentiation. Our data provide mechanistic insight into the endogenous regulators of human nervous system commitment, as well as a method for deriving neural cells from hPSCs with minimal cytokine and drug exposure. In addition, because of its rapid expression profile during neural differentiation, NPTX1 may be used in combination with other methods (Bock et al., 2011; Boulting et al., 2011) to help predict the ability of hPSC lines to differentiate toward the neural lineage.

EXPERIMENTAL PROCEDURES

Cell Culture Conditions

hESCs (WA-09, passages 30–45), (WA-01, passages 35–45), and iPSC line 42 were cultured on mouse embryonic fibroblasts (MEFs; Global Stem) plated at 12–15,000 cells/cm^2 in Dulbecco's modified Eagle's medium/F12, 20% KSR (GIBCO), 0.1 mM b-mercaptoethanol, NEAA (GIBCO), and 10 ng/ml FGF-2 (R&D). For some cultures, hESCs were maintained using StemBeads FGF-2 (StemCulture). Cells were passaged using 6 U/ml of dispase in hESC media, washed, and replated at a dilution of 1:10.

Neural Induction

Feeder-free neural induction was carried out as previously described (Chambers et al., 2009). Briefly, hPSC cultures were disaggregated using Accutase for 20 min, washed with hPSC media, and preplated on gelatin for 1 hr at 37°C in the presence of ROCK inhibitor to remove MEFs. The nonadherent hPSCs were washed and plated at a density of 20,000 cells/cm^2 on Matrigel (BD)-coated dishes in MEF conditioned hESC media (CM) spiked with 10 ng/ml of FGF-2 and ROCK inhibitor. The next day, the ROCK inhibitor was withdrawn and the hESCs were allowed to expand in the CM for 3 days or until they were nearly confluent. The initial differentiation media conditions included KSR media with 10 nM TGF-β inhibitor (SB431542; Tocris) and 500 ng/ml of Noggin (R&D) or LDN 193189 (STEMGENT). Upon day 5 of differentiation, increasing amounts of N2 media (25%, 50%, and 75%) were added to the KSR media every 2 days while maintaining 500 ng/ml of Noggin and TGF-β inhibitor. For TDGF1 antibody (ABCAM) experiments, antibody was added at 1 μg/ml.

Lentiviral Constructs

A third-generation lentiviral vector (Lois et al., 2002) was modified to express *NPTX1* shRNAs from the H1 promoter as previously described (Fasano et al., 2007). A list of the shRNA sequences is provided in the Supplemental Experimental Procedures. For overexpression, the NPTX1 open reading frame (ORF) was cloned by PCR using a bacterial clone template (Open Bio-Systems). The ORF was then placed into a lentiviral vector coexpressing GFP (SBI Biosciences). Viral particles were generated as previously described (Fasano et al., 2007).

Molecular Analyses

Total RNA was extracted using the RNeasy kit and DNase I treatment (-QIAGEN), and reverse transcribed (QuantiTect; QIAGEN). For qRT-PCR, Taqman probes (ABI) were used according to the manufacturer's protocols and run on a Realplex2 system (Eppendorf). Normalized Ct values were calculated as previously described (Fasano et al., 2010). Details regarding the microarray methods can be found in the Supplemental Experimental Procedures. The microarray CEL files have been submitted to Gene Expression Omnibus (GEO; GSE34551).

Immunocytochemistry

Cells were fixed in 4% paraformaldehyde, permeabilized with Triton X-100-containing buffer, and stained with primary antibodies (a list of the antibodies used is provided in Supplemental Experimental Procedures). Appropriate fluorescent-labeled secondary antibodies (Molecular Probes) and DAPI counterstaining was used for visualization.

ACCESSION NUMBERS

The microarray CEL files have been submitted to GEO under accession number GSE34551.

SUPPLEMENTAL INFORMATION

Supplemental Information includes Supplemental Experimental Procedures, seven figures, and six tables and can be found with this article online at http://dx.doi.org/10.1016/j.celrep.2014.01.026.

AUTHOR CONTRIBUTIONS

N.B. performed microarray analysis, all biochemical assays, and FACS analyses, and assisted with data interpretations and writing of the manuscript. S.E.H. maintained hESC lines, performed neural differentiations and qRT-PCR, and assisted with data interpretation and editing of the manuscript. S. Le generated all lentiviral constructs and performed qRT-PCR. B.C. generated, characterized, and differentiated iPSC lines, and performed endoderm and mesoderm differentiations. F.N. performed mouse epiblast stem cell experiments. S. Lotz performed FACS analyses. A.P.M. helped maintain hPSC lines. Q.W. assisted with IP and protein analyses. N.T. performed NPTX1 control experiments. P.J.T. supervised F.N. and helped with data interpretation and manuscript preparation. C.A.F. designed and supervised execution of the entire study, performed initial neural differentiations, assisted with data interpretation and analysis, and wrote the manuscript.

ACKNOWLEDGMENTS

We thank Susan Goderie for technical assistance, Paul Worley for providing the NPTX1 antibody, and Joseph Fasano, Karen Kirchofer, and Sally Temple for critical readings of the manuscript. This work was supported by grants from the NYSTEM program (C024177 and C024298), NINDS (NS072434-01A1), and the Regenerative Research Foundation.

Received: November 19, 2012
Revised: December 6, 2013
Accepted: January 17, 2014
Published: February 13, 2014

REFERENCES

Bjartmar, L., Huberman, A.D., Ullian, E.M., Rentería, R.C., Liu, X., Xu, W., Prezioso, J., Susman, M.W., Stellwagen, D., Stokes, C.C., et al. (2006). Neuronal pentraxins mediate synaptic refinement in the developing visual system. J. Neurosci. *26*, 6269–6281.

Blagosklonny, M.V. (2004). Do cells need CDK2 and ... Bcr-Abl? Cell Death Differ. *11*, 249–251.

Bock, C., Kiskinis, E., Verstappen, G., Gu, H., Boulting, G., Smith, Z.D., Ziller, M., Croft, G.F., Amoroso, M.W., Oakley, D.H., et al. (2011). Reference Maps of human ES and iPS cell variation enable high-throughput characterization of pluripotent cell lines. Cell *144*, 439–452.

Boulting, G.L., Kiskinis, E., Croft, G.F., Amoroso, M.W., Oakley, D.H., Wainger, B.J., Williams, D.J., Kahler, D.J., Yamaki, M., Davidow, L., et al. (2011). A functionally characterized test set of human induced pluripotent stem cells. Nat. Biotechnol. *29*, 279–286.

Brown, S., Teo, A., Pauklin, S., Hannan, N., Cho, C.H., Lim, B., Vardy, L., Dunn, N.R., Trotter, M., Pedersen, R., and Vallier, L. (2011). Activin/Nodal signaling controls divergent transcriptional networks in human embryonic stem cells and in endoderm progenitors. Stem Cells *29*, 1176–1185.

Casellas, R., and Brivanlou, A.H. (1998). Xenopus Smad7 inhibits both the activin and BMP pathways and acts as a neural inducer. Dev. Biol. *198*, 1–12.

Chambers, S.M., Fasano, C.A., Papapetrou, E.P., Tomishima, M., Sadelain, M., and Studer, L. (2009). Highly efficient neural conversion of human ES and iPS cells by dual inhibition of SMAD signaling. Nat. Biotechnol. *27*, 275–280.

Chen, C., and Shen, M.M. (2004). Two modes by which Lefty proteins inhibit nodal signaling. Curr. Biol. *14*, 618–624.

Chng, Z., Teo, A., Pedersen, R.A., and Vallier, L. (2010). SIP1 mediates cell-fate decisions between neuroectoderm and mesendoderm in human pluripotent stem cells. Cell Stem Cell *6*, 59–70.

Cho, R.W., Park, J.M., Wolff, S.B., Xu, D., Hopf, C., Kim, J.A., Reddy, R.C., Petralia, R.S., Perin, M.S., Linden, D.J., and Worley, P.F. (2008). mGluR1/5-dependent long-term depression requires the regulated ectodomain cleavage of neuronal pentraxin NPR by TACE. Neuron *57*, 858–871.

D'Andrea, D., Liguori, G.L., Le Good, J.A., Lonardo, E., Andersson, O., Constam, D.B., Persico, M.G., and Minchiotti, G. (2008). Cripto promotes A-P axis specification independently of its stimulatory effect on Nodal autoinduction. J. Cell Biol. *180*, 597–605.

Fasano, C.A., Dimos, J.T., Ivanova, N.B., Lowry, N., Lemischka, I.R., and Temple, S. (2007). shRNA knockdown of Bmi-1 reveals a critical role for p21-Rb pathway in NSC self-renewal during development. Cell Stem Cell *1*, 87–99.

Fasano, C.A., Chambers, S.M., Lee, G., Tomishima, M.J., and Studer, L. (2010). Efficient derivation of functional floor plate tissue from human embryonic stem cells. Cell Stem Cell *6*, 336–347.

Hemmati-Brivanlou, A., and Melton, D.A. (1994). Inhibition of activin receptor signaling promotes neuralization in Xenopus. Cell *77*, 273–281.

James, D., Levine, A.J., Besser, D., and Hemmati-Brivanlou, A. (2005). TGFbeta/activin/nodal signaling is necessary for the maintenance of pluripotency in human embryonic stem cells. Development *132*, 1273–1282.

Kennedy, M., D'Souza, S.L., Lynch-Kattman, M., Schwantz, S., and Keller, G. (2007). Development of the hemangioblast defines the onset of hematopoiesis in human ES cell differentiation cultures. Blood *109*, 2679–2687.

Kirkpatrick, L.L., Matzuk, M.M., Dodds, D.C., and Perin, M.S. (2000). Biochemical interactions of the neuronal pentraxins. Neuronal pentraxin (NP) receptor binds to taipoxin and taipoxin-associated calcium-binding protein 49 via NP1 and NP2. J. Biol. Chem. *275*, 17786–17792.

Levine, A.J., and Brivanlou, A.H. (2007). Proposal of a model of mammalian neural induction. Dev. Biol. *308*, 247–256.

Lois, C., Hong, E.J., Pease, S., Brown, E.J., and Baltimore, D. (2002). Germline transmission and tissue-specific expression of transgenes delivered by lentiviral vectors. Science *295*, 868–872.

Lonardo, E., Parish, C.L., Ponticelli, S., Marasco, D., Ribeiro, D., Ruvo, M., De Falco, S., Arenas, E., and Minchiotti, G. (2010). A small synthetic cripto blocking Peptide improves neural induction, dopaminergic differentiation, and functional integration of mouse embryonic stem cells in a rat model of Parkinson's disease. Stem Cells *28*, 1326–1337.

Najm, F.J., Chenoweth, J.G., Anderson, P.D., Nadeau, J.H., Redline, R.W., McKay, R.D., and Tesar, P.J. (2011). Isolation of epiblast stem cells from preimplantation mouse embryos. Cell Stem Cell *8*, 318–325.

Nostro, M.C., Sarangi, F., Ogawa, S., Holtzinger, A., Corneo, B., Li, X., Micallef, S.J., Park, I.H., Basford, C., Wheeler, M.B., et al. (2011). Stage-specific signaling through TGFβ family members and WNT regulates patterning and pancreatic specification of human pluripotent stem cells. Development *138*, 861–871.

Patani, R., Compston, A., Puddifoot, C.A., Wyllie, D.J., Hardingham, G.E., Allen, N.D., and Chandran, S. (2009). Activin/Nodal inhibition alone accelerates highly efficient neural conversion from human embryonic stem cells and imposes a caudal positional identity. PLoS ONE *4*, e7327.

Piccolo, S., Agius, E., Leyns, L., Bhattacharyya, S., Grunz, H., Bouwmeester, T., and De Robertis, E.M. (1999). The head inducer Cerberus is a multifunctional antagonist of Nodal, BMP and Wnt signals. Nature *397*, 707–710.

Reynolds, B.A., and Weiss, S. (1992). Generation of neurons and astrocytes from isolated cells of the adult mammalian central nervous system. Science *255*, 1707–1710.

Smith, J.R., Vallier, L., Lupo, G., Alexander, M., Harris, W.A., and Pedersen, R.A. (2008). Inhibition of Activin/Nodal signaling promotes specification of human embryonic stem cells into neuroectoderm. Dev. Biol. *313*, 107–117.

Tesar, P.J., Chenoweth, J.G., Brook, F.A., Davies, T.J., Evans, E.P., Mack, D.L., Gardner, R.L., and McKay, R.D. (2007). New cell lines from mouse epiblast share defining features with human embryonic stem cells. Nature *448*, 196–199.

Vallier, L., Reynolds, D., and Pedersen, R.A. (2004). Nodal inhibits differentiation of human embryonic stem cells along the neuroectodermal default pathway. Dev. Biol. *275*, 403–421.

Vallier, L., Mendjan, S., Brown, S., Chng, Z., Teo, A., Smithers, L.E., Trotter, M.W., Cho, C.H., Martinez, A., Rugg-Gunn, P., et al. (2009). Activin/Nodal signalling maintains pluripotency by controlling Nanog expression. Development *136*, 1339–1349.

Weinstein, D.C., and Hemmati-Brivanlou, A. (1999). Neural induction. Annu. Rev. Cell Dev. Biol. *15*, 411–433.

Xu, R.H., Peck, R.M., Li, D.S., Feng, X., Ludwig, T., and Thomson, J.A. (2005). Basic FGF and suppression of BMP signaling sustain undifferentiated proliferation of human ES cells. Nat. Methods *2*, 185–190.

Yeo, C., and Whitman, M. (2001). Nodal signals to Smads through Cripto-dependent and Cripto-independent mechanisms. Mol. Cell *7*, 949–957.

Zhang, X., Huang, C.T., Chen, J., Pankratz, M.T., Xi, J., Li, J., Yang, Y., Lavaute, T.M., Li, X.J., Ayala, M., et al. (2010). Pax6 is a human neuroectoderm cell fate determinant. Cell Stem Cell *7*, 90–100.